Chinese Chemical Letters 34 (2023) 108457

Contents lists available at ScienceDirect

Chinese Chemical Letters

journal homepage: www.elsevier.com/locate/cclet

Solid–liquid-core optical fiber biosensor for highly sensitive and selective detection of 4-chlorophenol in water

Cangxu Feng[a,b], Jianwei Zhang[a], Chao Bian[a,b,*], Linyang Li[b], Rong Hu[b], Haixing Chang[c], Fei Peng[b], Xiaofeng Peng[b,*], Nianbing Zhong[b,*]

[a] Center for Hydrogeology and Environmental Geology Survey, China Geological Survey, Baoding 071051, China
[b] Intelligent Fiber Sensing Technology of Chongqing Municipal Engineering Research Center of Institutions of Higher Education, Chongqing Key Laboratory of Modern Photoelectric Detection Technology and Instrument, Chongqing Key Laboratory of Fiber Optic Sensor and Photodetector, Chongqing University of Technology, Chongqing 400054, China
[c] School of Chemistry and Chemical Engineering, Chongqing University of Technology, Chongqing 400054, China

ARTICLE INFO

Article history:
Received 23 November 2022
Revised 8 March 2023
Accepted 14 April 2023
Available online 15 April 2023

Keywords:
4-Chlorophenol
Solid–liquid-core optical fiber
Horseradish peroxidase
Permselective polymer membrane
Sensitivity
Selectivity

ABSTRACT

A novel solid–liquid-core fiber-optic biosensor was fabricated for highly sensitive and selective detection of 4-chlorophenol in water. The sensor comprised horseradish peroxidase (HRP)-coated U-shaped liquid-core optical fiber (LCOF) and 4-chlorophenol permselective polymer membrane. The U-shaped LCOF was filled with ethanol suspension of SiO_2 particles and the polymer membrane was composed of molecularly imprinted polymer, sulfonated polyethersulfone, and polysulfone. The morphology, composition, and surface luminous properties of the sensing region were examined. The effects of the diameter and content of SiO_2 particles and temperature of 4-chlorophenol solutions on the sensitivity of the biosensors were investigated. Further, the sensitivity, selectivity, response time, and limit of detection (LOD) of the biosensors was investigated. In addition, the effects of fiber core materials on the light transmission in sensing region were investigated and a biosensor sensing model was established. The proposed sensor exhibited high selectivity for 4-chlorophenol with satisfactory sensitivity, LOD, and response time: -1.18 $(\mu g/L)^{-1}$, 30 μg/L, and 400 s, respectively. The results are expected to aid in the development of methods for enhancing sensitivity of fiber-optic sensors and surface luminous intensity of optical fibers.

4-Chlorophenol (4-CP) is an important chlorophenol widely used in the industrial production of pesticides, drugs, dyes, and plastics [1]. 4-CP is highly toxic, carcinogenic, persistent, and biodegradable [2], and poses a serious threat to water ecological security and human health [3–5]. Therefore, the design and fabrication of online sensors for accurate quantification of the 4-CP concentration in wastewater is crucial for both the aquatic environment and human health.

To realize online detection of the concentration of 4-CP and phenolic compounds, electrochemical, photoelectrochemical, and fiber-optic sensors have been exploited [2,6–8]. Among online methods, fiber-optic sensors, such as surface plasmon resonance (SPR) fiber biosensors [9], long-period fiber grating (LPFG) biosensors [10,11], photochemical fiber-optic sensors [11,12], and optic-fiber evanescent wave (EW) sensors [7,11,12], have emerged as alternatives for the detection of phenolic compounds. In particular, the reported optical fiber sensors rely on photocatalytic or enzymatic reactions between photocatalysts or enzymes and phenolic compounds to form soluble products such as catechol, *o*-quinone, and melanin [11–14]. Soluble byproducts exhibit a higher refractive index (RI) than their monomeric precursors, thus increasing the RI of the solution [11,12]. Consequently, the transmitted light intensity or center wavelength of the absorption spectrum of the fiber sensors is changed [7,11,15], enabling the detection of phenolic compounds. However, fiber-optic sensors still experience the critical problem of low sensitivity [7,11,12,16]. The unsatisfactory sensitivity is due to the low light intensity of the solid optical fibers on the unclad surface, because the fibers with normal core-clad structures with core-clad waveguides provide very low SPR/LSPR excitation light at the surface of the fiber [16,17]. Therefore, enhancing the effective excitation light for analytes using fibers with standard core-clad structures is challenging.

This study proposed a simple strategy for enhancing the luminous intensity on the fiber surface using hollow capillary optical fibers (HCOFs). Subsequently, a novel solid-liquid-core optical fiber (S–LCOF) biosensor for the highly sensitive and selective

* Corresponding authors.
E-mail addresses: chao_bian@126.com (C. Bian), pxf@cqut.edu.cn (X. Peng), pxlb08@cqut.edu.cn (N. Zhong).

https://doi.org/10.1016/j.cclet.2023.108457
1001-8417/

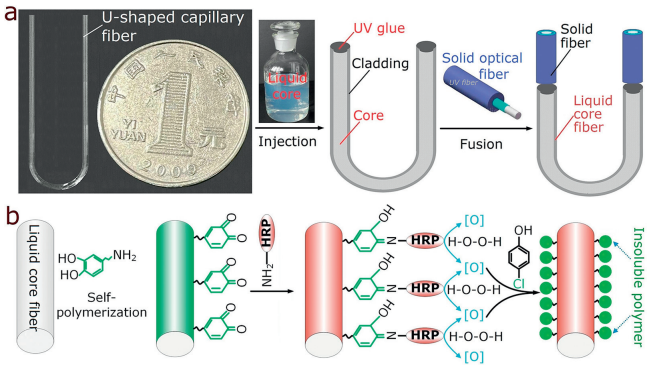

Fig. 1. Schematic of sensor fabrication: (a) preparation of U-shaped solid–HCOFs and (b) fabrication of HRP-coated U-shaped optical fibers.

detection of 4-chlorophenol based on U-shaped HCOFs was fabricated, as shown in Fig. 1. The biosensor was based on horseradish peroxidase (HRP)-coated U-shaped liquid-core optical fiber (LCOF) and molecularly imprinted polymer (MIP)-copolymer (sulfonated polyethersulfone and polysulfone, SPP) membranes. Further, the U-shaped LCOFs was filled with an ethanol suspension of SiO_2 particles (ESSP).

The preparation of U-shaped S–LCOFs and solid quartz optical fibers (SOFs), HRP-coated U-shaped optical fibers, and 4-CP selective permeation membranes is shown in Section S1 (Supporting information). The material characterization, preparation of the analytical solution, and test system and operation are presented in Sections S2-S4 (Supporting information). The measurement system is shown in Fig. S1 (Supporting information). The theoretical model of the biosensors is presented in Section S5 (Supporting information). The light transmission models in the U-shaped SOF and U-shaped S–LCOFs with pure ethanol and ESSP are shown in Fig. S2 (Supporting information).

The FESEM images of the SiO_2 particles with a micro-nano spherical structure (average diameter: 0.5, 1.0, 2.0, and 3.0 μm) are shown in Figs. S3a-d (Supporting information). Fig. S3e (Supporting information) shows that the SiO_2 particles were uniformly dispersed in ethanol, and the ESSP displayed high light transmittance. LCOF with clean and smooth surfaces are shown in Figs. 2a and b, respectively. The surface elements were Si and O (Fig. S4a in Supporting information). Images of the fiber exhibiting a rough surface with polydopamine particles after polydopamine polymerization are shown in Figs. 2c and d. The elements on the fiber surface changed to Si, O, C, and N; the newly added elements, C and N, on the fiber surface originated from polydopamine (Fig. S4b in Supporting information). This illustrates that dopamine self-polymerizes and coats the surface of the optical fiber. The surface morphology of the HRP-coated fibers is shown in Figs. 2e and f. Comparing the foregoing with the image in Fig. 2d, the surface roughness of the fiber increased because the HRP enzyme was immobilized on the polydopamine surface. Upon comparing Fig. S4b with Fig. S4c (Supporting information), Fe is observed to have been added owing to the HRP containing this element. This indicates that HRP was immobilized on the fiber. A new insoluble polymer coated the fiber surface (Figs. 2g and h). Furthermore, by comparing Fig. S4c with Fig. S4d (Supporting information), the Cl from 4-CP was exposed. Thus, it can be concluded that HRP catalysis of 4-CP resulted in the generation of insoluble chlorine-containing polyaromatic products on the surface. Fig. S5 (Supporting information) further confirms that the improved surface roughness in Figs. 2g and h is because of the production of new insoluble products during HRP catalysis of 4-CP instead of the molecular absorption of 4-CP. FESEM images of the MIP–SPP membrane with a rough surface due to the MIP microspheres (diameter: 1–2 μm) are shown in Figs. 2i and j.

The luminescence characteristics and sensitivity of the sensors without HRP coating were experimentally studied, and the results showed that the luminance of the U-shaped LCOF filled with an ethanol suspension of 0.5 μm SiO_2 particles was the highest (Fig. 3a). The reasons for this are as follows. First, the RI of the cladding is higher than that of the fiber core (RIs of air, ethanol, and SiO_2 are, respectively, 1.00, 1.362 and 1.451) [4,18]. The increase in the RI of the fiber core to that of the cladding improved the light transmission modes and induced light beams into the fiber cladding *via* refraction at the core-cladding interface. Furthermore, when the sensing region was converted to an LCOF, light rays, I_{in}, were refracted into the liquid core at the interface between the SOF and LCOF (Section S5); thus, the quality of the surface luminous spectrum of HCOF and S–LCOFs was better than that of the SOFs. Second, the RI of ethanol is higher than that of air, which enhanced the transmission of light inside the fiber, resulting in a high light intensity in the U-shaped region of the fiber core. Third, SiO_2 particles can induce light scattering [19], resulting in high light-scattering efficiency in the fiber core and high luminous power. Fourth, the light scattering intensity decreases with increasing SiO_2 diameter [20].

Fig. 3b shows that the luminous intensity from the U-shaped SOF surface exhibited the lowest level because the emitted intensity was based on the evanescent field [19,21,22]. The U-shaped HCOF exhibited an abnormally high attenuation coefficient, and even the luminous intensity was lower than that of the U-shaped S–LCOF after 20 mm. This is because the RI difference between the air core and the silica cladding is too large, and a large propagation loss is caused by the refraction and evanescent field when the fiber length is less than 20 mm; however, when the length is more than 20 mm, the luminous intensity at the fiber surface is based on the evanescent field. Moreover, close to the U-shaped region, the luminous intensity increases because of internal light reflection in the U-shaped region [4,19]. Furthermore, the highest luminous light intensity of the U-shaped LCOF filled with 0.5 μm SiO_2 particles occurred because of the highest light scattering intensity.

Fig. 3c shows that the U-shaped S–LCOF filled with ethanol suspension of 1.0 μm SiO_2 particles exhibited the highest sensitivity of -0.033 $(\mu g/L)^{-1}$, which is 3.60 and 2.19 times that of the SOF sensor and U-shaped sensor, respectively. The reasons for this are as follows. First, S–LCOF exhibited a high surface luminous intensity. Second, although the surface luminous intensity of the fibers with 0.5 μm SiO_2 particles was higher than that of the fibers with 1.0 μm SiO_2 particles, the forward scattering, which is an important factor for improving the sensitivity of the sensor, decreased with increasing SiO_2 particle size [20]. Third, the number of SiO_2 particles decreased with an increase in their size when the SiO_2 content is constant, which decreased N (N is the number of scattering times of light passing through the SiO_2 microspheres.) (Section S5). Fourth, the scattering angle (β) decreased with increasing SiO_2 particle diameter. Eq. S13 (Supporting information) shows that the sensitivity of the sensor decreased with decreasing N and β.

In Fig. S6 (Supporting information), the U-shaped S–LCOFs exhibited good sensitivity corresponding to a high luminous light intensity when the fiber core was filled with an ethanol suspension of 2.5% w/v 1.0 μm SiO_2 particles. The highest sensitivity of the sensor occurred because of its high surface luminous intensity and large N.

The shapes of the transmission spectra of the U-shaped S–LCOF with and without HRP coating are similar, as shown in Fig. 4a. However, the amplitude was ordered as follows: uncoated fiber in the absence of H_2O_2 > HRP-coated fiber in the absence of H_2O_2 > HRP-coated fiber in the presence of H_2O_2. The reasons for this are as follows. The light beam incident on the surface of the fiber

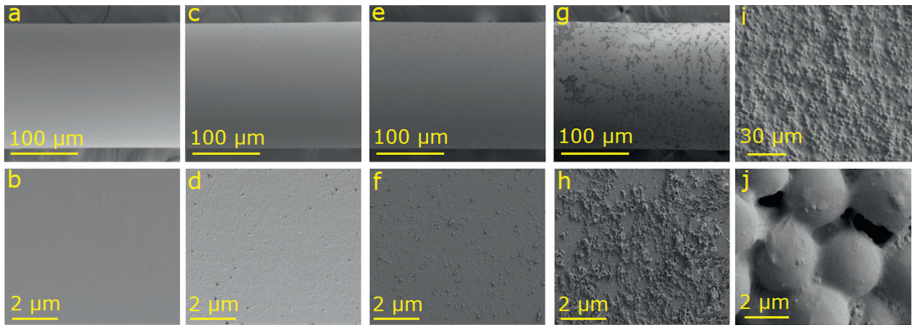

Fig. 2. FESEM images of fiber's sensing region: (a and b) LCOF, (c and d) polydopamine-coated S–LCOF, (e and f) HRP-coated S–LCOF, (g and h) insoluble polymer (4-CP oxidation product)-coated S–LCOF, and (i and j) MIP–SPP membrane.

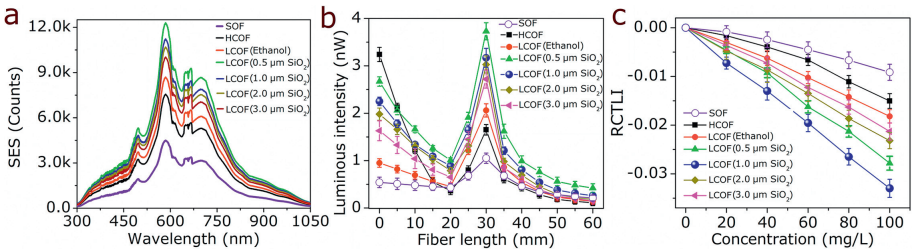

Fig. 3. Luminous characteristics of the sensing region and sensitivity of sensors: (a) the surface emission spectrum (SES) of the sensing region at fiber length 30 mm (the SiO_2 doping content in ethanol was 2.0% w/v), (b) surface luminous intensities in the sensing regions, and (c) sensitivity of sensors without HRP coating (4-CP temperature and pH are 20 °C and 7.4, respectively, and sample time is 630 s).

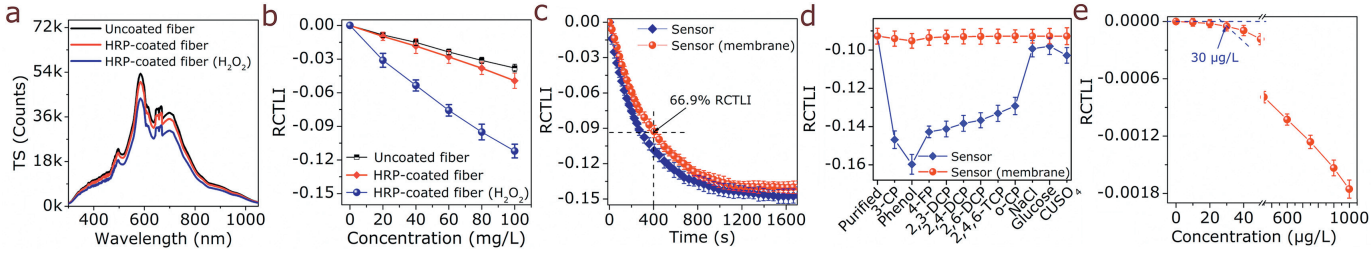

Fig. 4. Performance of U-shaped S–LCOF biosensor (SiO_2 diameter and doping content are 1 μm and 2.5% w/v, respectively; 4-CP temperature and pH are 20 °C and 7.4, respectively): (a) transmission spectrum (TS) in 100 mg/L 4-CP solution; (b) sensitivity of sensors (bare U-shaped S–LCOF sensor, HRP-coated S–LCOF sensor, HRP-coated S–LCOF sensor with H_2O_2 present; sample time is 630 s); (c) response time of sensor in 100-mg/L 4-CP solution (sample time is 630 s); (d) selectivity of sensor ("purified" means no other additives (*e.g.*, 3-CP, phenol, and 4-FP), sample time is 400 s); and (e) LOD of sensor (sample time is 400 s).

core entered and was absorbed by the HRP coating. Furthermore, the HRP coating had a higher RI than the 4-CP solution, resulting in a higher loss of transmitted light. Consequently, the quality of the transmission spectrum of the HRP-coated fibers was lower than that of the uncoated fibers. In particular, the quality of the transmission spectrum of the HRP-coated fiber decreased further in the presence of H_2O_2. This can be attributed to HRP-catalyzed 4-CP in the presence of H_2O_2 which can generate insoluble polymers and attach to the surface of the fiber (Figs. 2d and i). The polymer had a higher RI and rougher surface than that of the HRP coating. This increased the light scattering and absorption, which decreased the transmission quality of the optical fiber.

Fig. 4b shows that when the U-shaped sensing region was coated with HRP, the sensor exhibited a higher sensitivity because the HRP coating enhanced the molecular absorption of 4-CP. Moreover, when H_2O_2 was added to the 4-CP solution, the sensitivity increased significantly because both HRP and H_2O_2 contributed to the catalytic reaction of 4-CP and produced an insoluble polymer. The insoluble polymer enhanced the luminous light absorption and light scattering at the interface between the fiber and coating. Therefore, the HRP enzyme-catalyzed reaction of 4-CP to produce insoluble products can significantly improve the sensitivity of the U-shaped S–LCOF sensors.

The effect of the temperature of 4-CP solution on the sensor sensitivity was further investigated. The experimental results are shown in Fig. S7 (Supporting information), and it can be seen from the figure that when the temperature was 25 °C, the sensor sensitivity reached its highest value (-1.28 (μg/L)$^{-1}$), which was 2.29 and 13.99 times higher than that of our previously reported [7] and U-shaped solid–fiber-optic sensors, respectively. The reasons for this are as follows. First, the RIs decreased from the core of the SOF to that of the LCOF, that is, $n_1 > n'_1$; the RIs increased from the liquid core to the cladding, that is, n'_1 (n''_1) $< n'_2$ (Section S5); and the doped SiO_2 in the liquid core enhanced light scattering, which changed the light transmission modes in the sensing region and increased the surface luminous intensity of the S-LCOF sensor. Second, the activity of the HRP enzyme reached its highest level at 25 °C and pH 7.4, and the rate of movement of 4-CP molecules at 25 °C was acceptable; this supported the attainment of the highest insoluble product yield during the sensor sample time; accordingly, the sensor exhibited the highest sensitivity and lowest transmitted light intensity (Fig. S7).

The relative change in the transmitted light intensity (RCTLI, see Section S4) values of the sensor accurately tracing the dynamic process of the 4-CP response with the catalytic reaction time are shown in Fig. 4c. The sensor response with the SPM lagged behind

that of the sensor with no SPM because of the mass transfer resistance of the SPM to 4-CP transport. Although the sensor with SPM exhibited a delayed response to 4-CP, the sensitivity (-1.18 $(\mu g/L)^{-1}$) at a sample time of 630 s for the sensor with SPM only had a 9.2% loss relative to the sensor without SPM. This can be attributed to the following factors. First, SPM has high permeability to 4-CP [7]. Second, the eluent rapidly elutes the 4-CP adsorbed by SPM and transports it to the fiber surface [7]. Subsequently, insoluble polymers were generated and coated on the fiber surface owing to the catalytic reaction between HRP and 4-CP in the presence of H_2O_2. Furthermore, when the sensor adoption time was 400 s (*i.e.*, the catalytic reaction time was 400 s), the sensor sensitivity (-0.93 $(\mu g/L)^{-1}$) was 1.66 and 10.16 times higher than that of our previously reported [7] and U-shaped SOF sensors, respectively, reaching 66.9% of stable sensitivity. In addition, the sensor also demonstrated high-repeatability (Fig. S8 in Supporting information). Thus, for the measurements, a sampling time of 400 s was sufficient.

The sensor without SPM exhibited strong sensitivity fluctuations when other analytes were added to the 4-CP solution in the presence of H_2O_2 (Fig. 4d). The addition of phenolic compounds had the greatest impact on the sensitivity of the sensor because HRP enzymes could oxidize most phenolic compounds to insoluble polymers; HRP enzymes also exhibited the fastest selective oxidation of phenol. Consequently, when 100-mg/L phenol was added to the 100-mg/L 4-CP solution, the most significant change was observed in sensor sensitivity. Other compounds such as NaCl, glucose, and $CuSO_4$ do not catalyze HRP enzymes to generate new products. Nevertheless, their addition also changed the composition and RI of the 4-CP solution and enhanced the surface luminous light absorption intensity on the surface of the optical fiber, thus modifying the sensor sensitivity. This illustrates that the SPR-coated fiber-optic sensor without SPM does not enable the selective measurement of 4-CP in water. Moreover, the sensor with SPM exhibited slight sensitivity fluctuations to phenolic organics and no fluctuations to glucose molecules and ions. However, this was negligible compared to the response to 4-CP because the maximum relative error was only 3.6%. This high selectivity can be attributed to the MIP microspheres in the SPM with specific recognition of the 4-CP configuration. Thus, the highly selective adsorption and detection of 4-CP in water can be achieved using SPM.

Fig. 4e shows that the LOD, uncertainty, and maximum relative error of the sensor were 30 μg/L, less than 7.63%, and 7.4%, respectively. As summarized in Table S1 (Supporting information), the LOD of the sensor with the MIP–SPP membrane was equivalent to that of other methods for detecting 4-CP. These results reveal that the prepared HRP-coated S–LCOF biosensor with the MIP–SPP membrane can be used for the selective and sensitive detection of 4-CP in water, and can compete with other sensors in terms of sensitivity, selectivity, LOD, and response time.

In conclusion, a fiber-optic biosensor was fabricated by combining a U-shaped solid-liquid-core optic fiber, an HRP coating, and a polymer membrane. The developed biosensor overcome the fundamental problem of low sensitivity associated with SOF sensors with core-clad waveguides, which limits the effective surface luminous intensity in the sensing region, through the rapid oxidation of 4-CP using the HRP enzyme to form insoluble polymers in the presence of H_2O_2 with a high RI and strong light absorbance at the U-shaped surface. Furthermore, the fabricated biosensor resolved the problems of non-selectivity and high LOD of conventional fiber-optic sensors for the detection of 4-CP in water, and the high 4-CP permselectivity of the polymer membrane isolated the permeation of other phenol compounds, glucose molecules, and ions. It is expected that the proposed biosensor developed in this study can be used for accurately detecting 4-CP in water and promoting the engineering application of optical fiber sensors and enzyme-catalyzed reaction technologies.

Declaration of competing interest

There are no conflicts to declare.

Acknowledgments

The authors gratefully acknowledge the support from the National Natural Science Foundation of China (NSFC) (Nos. U19A20107, 52176178 and 51876018), Innovation Research Group of Universities in Chongqing (No. CXQT21035), Chongqing Natural Science Foundation Innovation and Development Joint Fund Project (No. CSTB2022NSCQ-LZX0059), and the Scientific and Technological Research Program of Chongqing Municipal Education Commission of China (No. KJZD-M202201101).

Supplementary materials

Supplementary material associated with this article can be found, in the online version, at doi:10.1016/j.cclet.2023.108457.

References

[1] N. Zhong, J. Yuan, Y. Luo, et al., Chem. Eng. J. 425 (2021) 130666.
[2] P. Yan, D. Jiang, H. Li, et al., Sens. Actuators B: Chem. 279 (2019) 466–475.
[3] L. Peng, Y. Bian, X. Shen, et al., Chin. Chem. Lett. 31 (2020) 2871–2875T.
[4] A.A.L Beduk, N. Tashkandi, K.N. Salama, Sens. Actuators B: Chem. 314 (2020) 128026.
[5] L. Meng, Y. Qu, L. Jing, Chin. Chem. Lett. 32 (2021) 3265–3276.
[6] H. Karimi-Maleh, C.T. Fakude, N. Mabuba, G.M. Peleyeju, O.A. Arotiba, J. Colloid Interface Sci. 554 (2019) 603–610.
[7] X. Xin, H. Liu, N. Zhong, et al., Sens. Actuators B: Chem. 357 (2022) 131468.
[8] M.C. Alcudia-León, R. Lucena, S. Cárdenas, M. Valcárcel, J. Chromatogr. A 1218 (2011) 2176–2181.
[9] S. Singh, S.K. Mishra, B.D. Gupta, Sens. Actuators B: Chem. 186 (2013) 388–395.
[10] S.K. Mishra, K.S. Chiang, Opt. Laser Technol. 131 (2020) 106464.
[11] N. Zhong, M. Chen, H. Chang, et al., Sens. Actuators B: Chem. 273 (2018) 1744–1753.
[12] N. Zhong, M. Chen, Z. Wang, X. Xin, B. Li, Lab Chip 18 (2018) 1621–1632.
[13] M. Wagner, J.A. Nicell, Water Res. 36 (2002) 4041–4052.
[14] M. Sarno, M. Iuliano, Mater. Today Proc. 20 (2020) 74–81.
[15] Y. Wang, S.R. Kavanagh, I. Burgués-Ceballos, et al., Nat. Photonics 16 (2022) 235–241.
[16] N. Zhong, M. Zhao, L. Zhong, et al., Biosens. Bioelectron. 85 (2016) 876–882.
[17] M. Ibanescu, Y. Fink, S. Fan, E.L. Thomas, J.D. Joannopoulos, Science 289 (2000) 415–419.
[18] N. Zhong, X. Zhu, Q. Liao, Y. Wang, R. Chen, Opt. Lett. 38 (2013) 3115–3118.
[19] S. Li, Z. Peng, R.M. Leblanc, Anal. Chem. 87 (2015) 6455–6459.
[20] S. Li, M. Yuan, W. Zhuang, et al., Laser. Photonics Rev. 15 (2021) 2000480.
[21] N. Zhong, M. Zhao, Y. Li, Biomed. Opt. Express 7 (2016) 335–351.
[22] L.Z. Pesavento, L. De Maria, G. Alberti, N. Cennamo, Biosensors 11 (2021) 72.